Association of Fibronectin and Vinculin with Focal Contacts and Stress Fibers in Stationary Hamster Fibroblasts

IRWIN I. SINGER
Institute for Medical Research of Bennington, Bennington, Vermont 05201

ABSTRACT We have recently observed a transmembrane association between extracellular fibronectin (FN) fibers and elongated focal patches or fibers of vinculin (VN) in G_1-arrested stationary Nil 8 hamster fibroblasts, with double-label immunofluorescence microscopy (Singer and Paradiso, 1981, *Cell*. 24:481–492). We hypothesized that these FN-VN complexes might correspond to focal contacts, the membrane sites that are probably mainly responsible for attaching cells to their substrata, because vinculin is often localized in focal contacts. However, because fibronectin-vinculin associations may not be restricted to the substrate adhesive surface of the cell, it became necessary to determine whether some or all of the various kinds of FN-VN complexes which we described are in proximity to the substrate. Using interference reflection optics and double-label immunofluorescence microscopy for fibronectin and vinculin, many elongated (up to 38 μm) FN-VN associations were found to be strikingly coincident with focal contacts in the perinuclear area of extremely flattened arrested Nil 8 fibroblasts in 0.3% fetal bovine serum (FBS). In addition, the long FN-VN adhesion complexes were precisely aligned with the major phase-dense stress fibers observed at the ventral surfaces of these stationary cells with phase contrast microscopy. Fibronectin was neither associated with vinculin-containing focal contacts of Nil 8 cells cultured in medium with 5% FBS nor with vinculin-negative focal contacts located at the extreme edges of stationary cells arrested in 0.3% FBS. Our time-course experiments suggest that early FN-VN lacking-focal contacts, which form at the cellular margins, develop into mature substrate adhesion complexes containing both fibronectin and vinculin, localized in the major stress fibers at the centers of sessile fibroblasts.

At least two kinds of anchorage structures are probably involved in the attachment of cells to their substrate: focal contacts and close contacts (34). The close contacts are characterized by a substrate separation distance of ~ 30 nm and are usually associated with a loose microfilament meshwork (28, 34). Focal contacts represent the closest substrate approach (10–15 nm), and are always found at the distal ends of microfilament bundes or stress fibers (28, 34, 35). Close contacts appear to continuously advance and are predominant in spreading and moving cells, whereas the focal contacts are stationary during locomotion and become most numerous in completely spread cells and within confluent monolayers (14, 26, 35). The bulk of the evidence indicates that focal contacts are mainly responsible for cellular adhesion (1, 34).

A number of recent studies have provided information concerning the molecular organization of the focal contact. Because fibronectin (FN) is a pericellular glycoprotein that apparently mediates the adhesion of cells to substrates (25, 36, 39, 50), and because it is coincident with actin microfilament bundles on the ventral cell surface (30, 33), it was reasonable to hypothesize that FN is a constituent of focal contacts (33). In addition, a very close (8–20 nm) transmembrane relationship between individual fibronectin fibrils and actin microfilaments termed the fibronexus has been demonstrated with electron microscopy (44). The fibronexus is often associated with dense submembranous plaques resembling those reported previously (2, 29), which correspond to focal contacts (28). These findings also suggest that fibronectin may be a component of the focal contact. Furthermore, vinculin (VN), a protein isolated from chicken smooth muscle, has been localized within focal contacts

THE JOURNAL OF CELL BIOLOGY · VOLUME 92 FEBRUARY 1982 398-408
 · 0021-9525/82/02/0398/11 $1.00

at the ends of actin-microfilament bundles (11, 21, 22). We therefore studied the distribution of fibronectin and vinculin in doubly stained fibroblasts to determine if a transmembrane relationship exists between these two proteins. Many vinculin-containing focal patches and longer fibers were strikingly coincident with fibronectin fibers at the ventral surface of well-spread growth arrested cells (45), thus implicating fibronectin as a component of focal contacts under these conditions. However, because vinculin and fibronectin may also be co-localized at structures on the dorsal cell surface that are not focal contacts (11), it became necessary to determine which of the several types of fibronectin-vinculin associations that we observed (45) do in fact correspond to focal contacts. In the experiments reported here, combinations of interference reflection microscopy (IRM), phase microscopy, and double-label immunofluorescence microscopy were used to analyze relationships between fibronectin, vinculin, focal contacts, and stress fibers. We observed that fibronectin was indeed localized beneath vinculin-containing interference reflection-negative (dark) focal contacts in cultures arrested in G_1 by serum limitation. Also, both vinculin and fibronectin fibers were coincident with phase dense stress fibers that were dark with IRM in these sessile fibroblasts. However, FN was not coincident with many of the focal contacts of cells grown in higher serum concentrations, in agreement with the work of others (5, 6, 8, 13, 20).

MATERIALS AND METHODS

Cell Culture

Nil 8 hamster fibroblasts were propagated in antibiotic-free Eagle's minimal essential medium (MEM; Autopow, Flow Laboratories, Rockville, Md.) containing 10% fetal bovine serum (FBS) and 2 mM glutamine. Sparse cultures of well spread G_1-arrested cells were obtained by seeding 6×10^4 cells in 1 ml of MEM supplemented with 0.3% FBS onto glass cover slips in 16-mm-diameter Costar cluster plate wells (16, 38). Denser growing cultures were established as above by plating 1×10^5 cells per well in MEM containing 5% FBS. Growing and G_1-arrested Nil 8 cultures were fixed at 3, 6, 24, 48 and 72 h after seeding.

Fibronectin and Vinculin Antisera

Human plasma FN was isolated by affinity chromatography on a gelatin-Sepharose column (41), and vinculin was obtained from chicken gizzards via DEAE chromatography (19, 21). Both proteins were purified further with preparative polyacrylamide gel electrophoresis (37, 45). Fibronectin antibodies were produced in rabbits, and vinculin antibodies were produced in guinea pigs. Both antisera have been shown to be monospecific for their respective immunogens (45) by performing radioimmunoelectrophoresis against total Nil 8 cell protein using ^{125}I protein A as previously described (10).

Immunofluorescence

The cover-slip cultures were ifixed in 3.5% paraformaldehyde in 0.1 M sucrose and 0.1 M Na-cacodylate (pH 7.2), permeabilized with 0.1% Triton X-100, and doubly labeled simultaneously with fibronectin (1:75) and vinculin (1:25) antibodies as before (45). Controls consisted of mixtures of fibronectin antibodies plus preimmune guinea pig serum or vinculin antibodies with preimmune rabbit serum. Cells incubated with preimmune rabbit or guinea pig sera did not exhibit any stained extracellular fibers, or cytoplasmic focal patches, respectively (45). Fibronectin was visualized indirectly with fluorescein isothiocyanate (FITC) conjugated goat anti-rabbit IgG (Miles-Yeda Ltd., Rohovot, Israel), and vinculin was labeled with tetramethylrhodamine conjugated $F(ab')_2$ goat anti-guinea pig IgG (N. L. Cappel Laboratories, Inc., Cochranville, Pa.), applied as mixtures at final dilutions of 1:10. The stained cultures were mounted in PBS and sealed with Valap (35).

Microscopy

Double immunofluorescence analysis and interference reflection microscopy were performed on an American Optical epifluorescence microscope using a 100 times magnification planachromatic oil immersion objective lens illuminating numerical aperture [I.N.A.] = 1.25 was calculated using the smallest lens aperture diameter of 2 mm as described previously [34]). Fluorescein-selective fluorescence was obtained by refitting this microscope with Zeiss interference filters: a BP 485/20 nm exciter filter, and a 520- to 560-nm barrier filter (plus the existing 510-nm dichroic mirror). Rhodamine staining was visualized with the American Optical narrow band 546-nm exciter filter, an LP 590-nm barrier filter, and a 560-nm dichroic reflector. IRM images were obtained by modification of the method of Curtis (17) in which the 546-nm exciter filter was used in combination with the 520- to 560-nm barrier filter, the 510-nm reflector, and the 100 times magnification planachromatic objective lens. Photomicrographs were made on Kodak Tri-X pan film processed with Ethol Blue developer at an ASA of 2,000. Correlated double-immunofluorescence and phase contrast microscopy was performed on duplicate cover-slip cultures with a Zeiss laboratory microscope using a vertical illuminator, a 63 times magnification planapochromatic objective lens (NA = 1.4), the FITC selective filters listed above, and a green selective excitation filter combination for rhodamine staining. Images made on this microscope were recorded on Kodak Technical Pan Film 2415 and developed with D-19.

Composite Micrographs

Composite photomicrographs were produced for analysis of the correspondence between fibronectin or vinculin immunofluorescence, and interference reflection-negative focal contacts or phase-dense stress fibers. A high contrast transparency of the interference reflection or phase-contrast image was made on Kodalith Ortho Film processed with Kodalith developer. The transparency was placed on top of a slightly underprinted micrograph of the corresponding immunofluorescence pattern, and rephotographed with Kodak Panatomic-X film to construct the combination image. To directly compare immunofluorescent vinculin and fibronectin labeling patterns of the same cell by this method, the vinculin negative was reversed on Kodak Technical Pan film and a high contrast transparency was then produced on Kodalith Ortho film as before (45).

RESULTS

Possible Effects of Fixation and Permeabilization on the Interference Reflection Pattern

Because cells must be preserved and permeabilized for the long-term immunofluorescence microscopic study of intracellular proteins, it is necessary to determine whether these procedures alter their interference reflection pattern. Although others have found that aldehyde fixation and permeabilization do not drastically alter the IRM image (49), I was concerned that the disruption of the cell membrane by treatment with nonionic detergent might change the thickness of the layer of medium between the cell and the substrate which in part generates the interference pattern (17, 34) and consequently change the appearance of focal contacts. The IRM images of living Nil 8 cells were therefore compared with those of formaldehyde-fixed and Triton X-100 permeabilized fibroblasts prepared for immunofluorescence microscopy. As indicated in Fig. 1 *A* and *B*, such processing did not appreciably change the interference reflection pattern of Nil 8 fibroblasts. Both living and fixed G_1-arrested cells cultured in medium containing 0.3% FBS exhibited two kinds of focal contacts: oblong focal patches found mainly at the cellular margins, and thin linear streaks that were much longer (7–25 μm) and localized beneath the nuclear and perinuclear areas (Fig. 1 *A*, *B*). The peripheral plaquelike focal contacts are similar to those previously reported at the leading lamella of chick fibroblasts (34, 35) in which vinculin is localized (21) (Fig. 2). Long reflection-negative (dark) structures resembling the ones reported here appear to be coincident with stress fibers (34). When cells arrested in G_1 for 24 h or longer were studied with IRM and antivinculin immunofluorescence, these very long perinuclear focal contacts were labeled with bright vinculin-specific staining (matching arrowheads in Fig. 1 *B* and *C*). High levels of diffuse fluorescence were also observed in the perinuclear area of cells stained with vinculin antibodies (Fig. 1 *C*). Control cultures labeled with preimmune sera (45), and chick fibroblasts (21) or rat myotubes (7) stained with affinity purified antivinculin IgG,

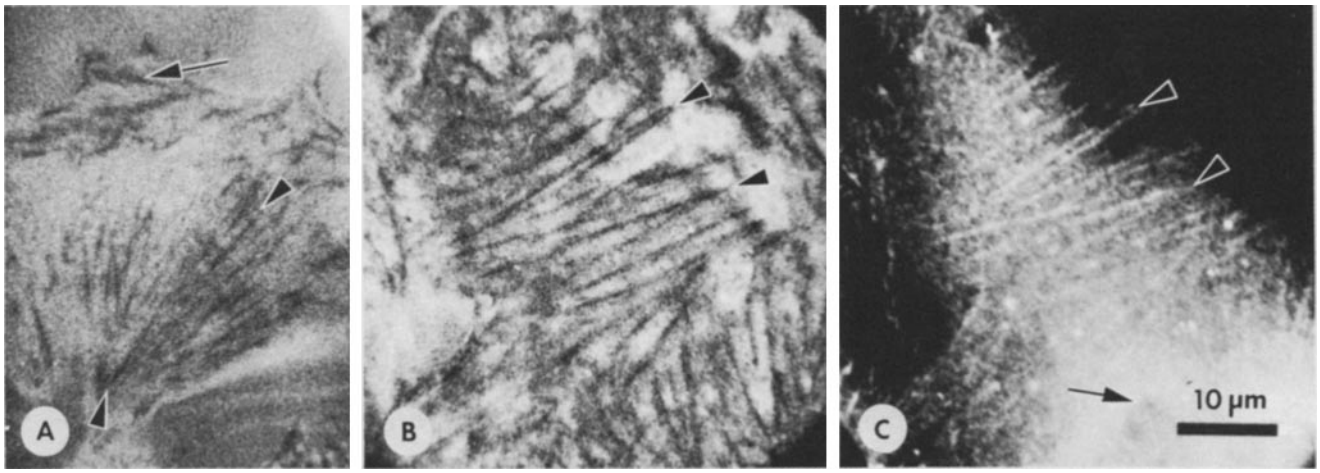

FIGURE 1 Interference-reflection and anti-vinculin immunofluorescence micrographs of sessile G_1-arrested Nil 8 cells cultured in 0.3% FBS for 24 h. (*A*) Living cell in culture medium under interference-reflection optics. Long thin focal contacts (arrowheads) are present at the cell center, whereas the typical oblong plaquelike focal contacts (arrow) are seen at the edge of the cell. (*B*) Interference-reflection micrograph of a well-spread Nil 8 cell fixed with 3.5% formaldehyde, permeabilized with 0.1% Triton X-100, and stained with anti-vinculin guinea pig antibodies as described in Materials and Methods. Many long fibrous focal contacts (arrowheads) similar to those in living untreated cells (*A*) are located in the nuclear and perinuclear areas. (*C*) Same field shown in (*B*) viewed with rhodamine fluorescence optics. The long fibrous focal contacts (arrowheads) are brightly stained by vinculin antibodies. Arrow indicates the edge of the nucleus. × 1400.

exhibited similar perinuclear backgrounds that could be removed by shearing away dorsal portions of the cells (7). These observations suggest that the diffuse perinuclear fluorescence is caused by a second dispersed (nonfibrous) distribution of vinculin, as well as by nonspecific adsorption of guinea pig IgG.

Fibronectin Fibers are Unrelated to Focal Contacts of Cells Cultured in 5% Serum

Nil 8 cells grown in medium containing 5% FBS were doubly stained with fibronectin plus vinculin antibodies and studied via indirect immunofluorescence, interference reflection, and phase-contrast microscopy, from 3 to 72 h after seeding. Their focal contacts were mainly of the shorter plaquelike variety and were usually excluded from the cell center (Fig. 2 *B*, and *E*). Most of these focal contacts were positively stained for vinculin (Fig. 2 *A*, and *B*, arrowheads), although a number of the contacts located at the cellular margin were conspicuously vinculin-negative (arrows in Figs. 2 *A* and *B*; arrowheads in 2 *D* and *E*). (In a recent analysis of the interference reflection image [23], Gingell described a series of concentric interference fringes which delineated the cellular periphery. He found that they were generated by the reduced thickness of the peripheral cytoplasm [<1 μm at an I.N.A. of 1.18] rather than by its membrane-to-substrate separation distance. Although I did not observe such series of continuous peripheral fringes, some short IR minima were seen parallel to the cellular margin [Fig. 2 *B*, crossed arrows]. Because these minima may be generated by the cell thickness, they were not interpreted as focal contacts in this analysis. Only the dark oblong focal patches whose long axes were oriented perpendicular to the cellular edge were considered to be focal contacts, as previously indicated [35]). Only a few prominent phase-dense stress fibers were seen in cells grown under these conditions (Fig. 2 *H*). Fibronectin fibers observed in the 6-h cultures were localized over the cellular centers and were not coincident with focal contacts (Fig. 2 *C*). Meshworks of curvilinear fibronectin fibers similar to those reported previously (38) were found closer to the periphery of the cell by 24 h, but these FN fibers did not coincide with focal contacts (arrowheads, Fig. 2 *F*). A few striae of fibronectin and vinculin were congruent with stress fibers in these cells (Fig. 2 *G* and *I*).

Correspondence of Fibers Showing Superimposition of Fibronectin and Vinculin Staining with Focal Contacts in G_1-Arrested Nil 8 Fibroblasts

In stark contrast to the cells cultured in 5% FBS, Nil 8 fibroblasts arrested in G_1 for a minimum of 24 h exhibited a striking coincidence of striated fibronectin and vinculin immunostaining with the long thin fiberlike focal contacts (Figs. 3 and 4). A composite photographic method (45) was used to demonstrate this impressive association. With this technique, the localization of vinculin (photographically reversed and shown in black) and fibronectin (shown in white) in doubly stained cells could be analyzed simultaneously to determine how precisely their patterns are interrelated (see VN·FN in Fig. 3 *D–F* and Fig. 4 *D–F*). Similarly, the relative distributions of the low-intensity reflections of focal contacts (in black) were correlated with the above fibronectin pattern (in white) (see IR·FN in Fig. 3 *J–L* and Figs. 4 *J–L*). To evaluate the fidelity with which this composite method reproduces the dimensions of structures in the original micrographs, coincident fibers from Figs. 3 and 4: *A–C*, *G–I*, and *M–O* were magnified 10 times and their widths determined with an ocular micrometer. When the same fibers were remeasured on the overlays and underlays, and these data were compared with the corresponding data from the original micrographs, either no change or a small increase in diameter was found. Using the high contrast overlays, I observed a mean size increase of 5.92% (range: 0 to 22%, n = 24). Similarly, a mean increase in width of 4.72% (range:

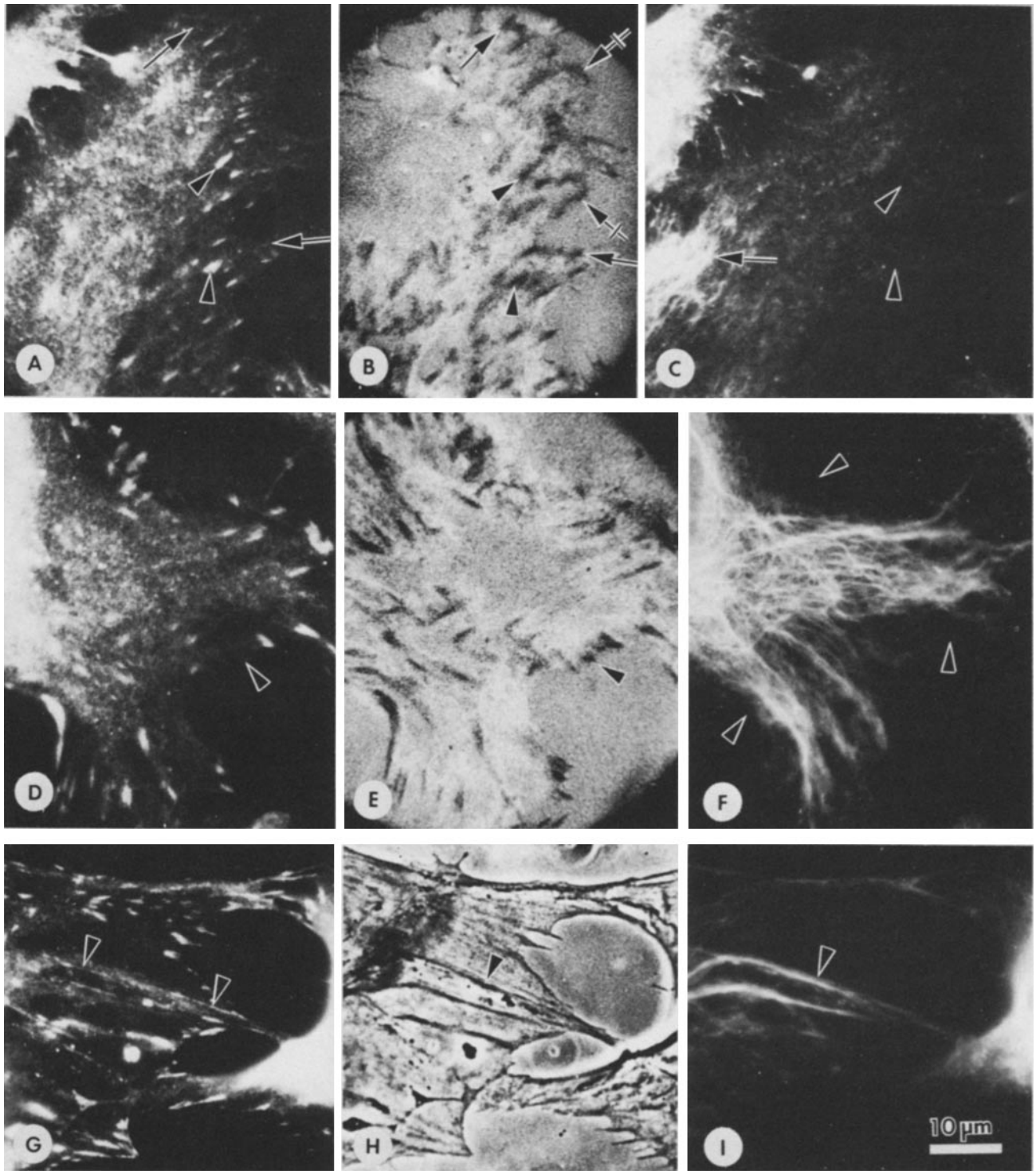

FIGURE 2 Correlated two chromophore immunofluorescence microscopy for vinculin (rhodamine, left column) and fibronectin (fluorescein, right column), and interference-reflection (*B*, *E*) and phase-contrast microscopy (*H*) of Nil 8 fibroblasts growing in 5% FBS. (*A–C*) cell fixed 6 h after seeding exhibits focal patches of vinculin (*A*, arrowheads) localized over focal contacts (*B*, arrowheads). Very long fibrous vinculin-containing focal contacts are absent from the cell center. Several focal contacts at the edge of the cell are vinculin negative (corresponding arrows, *A* and *B*). Crossed arrows in B show IRM minima that are probably not focal contacts. Clumps of fibronectin fibers located on the dorsal cell surface (*C*, arrow) do not overlap the areas containing focal contacts (*C*, corresponding arrowheads *A* and *B*). (*D–F*) Cell preserved after 24 h of culture in 5% FBS exhibits an increased amount of fibronectin fibers at the dorsal surface (*F*) that are not coincident with focal contacts (positions indicated by arrowheads in *F*). The distribution of vinculin is still punctate (*D*) and coincident with plaquelike focal contacts (*E*); some focal contacts at the edge of the cell are vinculin negative (corresponding arrowheads in *D* and *E*). (*G–I*) Same culture conditions as *D–F*. Phase micrograph reveals only a few stress fibers (*H*, arrowhead) that are coincident with striae showing vinculin (*G*, arrowheads) and fibronectin (*I*, arrowhead) immunolabeling. Most of the vinculin labeling is in short peripheral focal patches (*G*). × 1,200.

0 to 25%, n = 18) was obtained with the underlays. (In some instances, increases in fiber thickness appeared greater than the measured increase due to differences in contrast levels). Because the magnitude of the small increase in width determined for the overlay was not substantially different from the increase measured using the underlay, combining the two micrographs would not increase the apparent coincidence of fibronectin, vinculin, and focal contacts.

The most dramatic feature of these stationary fibroblasts was the coincidence of antifibronectin and antivinculin labeled striae with very long focal contacts that ranged up to 38 μm in length (arrows and arrowheads in Fig. 3, left and center columns; Fig 4, left column). Such triple-pattern associations were observed in 50 arrested cells fixed from 24 to 72 h after seeding. These elongated striae were usually arranged parallel to each other in groups situated at the ventral cell surface in the nuclear or perinuclear region (Fig. 3, left and center columns), and they closely resembled stress fibers (Fig. 5). To ensure that the long dark perinuclear focal contacts seen with IRM were not caused by the thinness of the perinuclear cytoplasm (23), it was necessary to determine this height. Cultures of Nil 8 cells were therefore fixed after 72 h of G_1 arrest and vertical sections were cut for electron microscopic study as previously outlined (44). Measurements of the distance between the edge of the nucleus and the point at which the thickness of the wedge-shaped cytoplasm was 1 μm in height were performed on electron micrographs. The mean of this distance was 8.17 μm ± 3.01 (SD) with a range of 5–16 μm (n = 21). The cytoplasmic thickness therefore exceeds the minimal requirement for an unambiguous measurement of cell-substrate separation via IRM (1 μm at an I.N.A. of 1.18 [23]; I used an I.N.A. of 1.25) for some distance from the nuclear edge (Fig. 1 *C*, arrow). Also, I did not observe any change in the IRM pattern (i.e., the appearance of fringes) at distances exceeding 16 μm from the nuclear margin that would be <1 μm thick (Fig. 1 *B*). Thus our IRM images most likely are patterns generated by variations in the thickness of the space between the cell and substrate.

The long dark perinuclear interference reflection minima (focal contacts) were either continuous (Figs. 1 *B*, 3 *M*; arrow, and 4 *M*) or interrupted by somewhat lighter regions at several points along their length (arrowheads in Fig. 3 *M* and *N*). In either case, the darkest areas were as black as the minima of the more typical focal contacts. The darkest regions of these long IR minima were also coincident with the brightest portions of the corresponding vinculin striae (matching arrowheads in Fig. 3 *A* and *M*; *B* and *N*), and the continuous dark streaks were nearly totally vinculin-positive (Figs. 1 *B* and *C*; 3 *A* and *M*; and 4 *A* and *M*). This evidence further suggests that the long streaky perinuclear minima are focal contacts because membrane-associated vinculin patches are usually localized in such adhesions (5, 21). The discontinuous streaks could represent an early stage in the formation of the continuous focal contacts.

Beginning at 48 h, fibers exhibiting a bright reflection were seen also (Fig. 3 *O*, short arrow); these were coincident with VN and/or FN immunofluorescence (Fig. 3, short arrows, right column). On occasion, reflection-negative (dark) FN-VN fibers abruptly became reflection-positive (bright) somewhere along their length (Fig. 3 *O*, long arrow), indicating that one end of this adhesion complex was close to the substrate while the other end was farther away. This increased separation from the substratum, perhaps caused by the buildup of fibronectin beneath the cell, was not seen as often as the dark fiberlike focal contacts.

If the coincidence of FN and VN was analyzed in double-labeled fibers beginning at their most centripetal position, one often observed that the fibronectin labeling was lost near the cellular margin whereas vinculin staining persisted there. Nevertheless, a weak (dark) interference reflection intensity was found along most of the length of the fiber (from the perinuclear area to the cell margin; Fig. 4 *e*'s in left column). These reflection minima closely resemble focal contacts, therefore indicating that the long doubly stained fibers coincident with them are closely opposed to the substrate for most of their length. Shorter focal contacts also exhibited very similar staining properties, depending upon their intracellular position. Those adhesions which were situated closest to the cell center were positive for both fibronectin and vinculin (Fig. 4, arrowheads in right column), whereas the focal contacts located between the perinuclear region and the cell margin were brightly stained by vinculin antisera but were mostly FN-negative even though their proximal ends overlapped fibronectin fibers (Fig. 3, arrowheads in right column; Fig. 4, long arrows in right column). Many focal contacts located at the margin of the cell showed neither fibronectin nor complete vinculin staining (Fig. 3 *A*, *C*, *M*, and *O*, crossed arrows show incomplete VN staining; Fig. 4, short arrows in left and right columns show focal contacts without VN). However, such peripheral focal contacts were both fibronectin- and vinculin-positive if FN fibers overlapped the edges of the cell (Fig. 4, center column).

Although a precise coincidence of FN, VN, and focal contacts was usually seen in our composite micrographs, a very close side-by-side apposition of fibronectin fibers and vinculin-containing focal contacts was sometimes observed (white arrowheads, Figs. 3 *D* and *J*, and 4 *D* and *J*). This orientation is similar to that reported previously (8).

FIGURE 3 Coincidence of anti-vinculin (*VN* in *A–C*) and anti-fibronectin (*FN* in *G–I*) immunofluorescent localization patterns with focal contacts seen in interference-reflection micrographs (*IR* in *M–O*) of well-spread growth-arrested Nil 8 cells fixed 24 h (left and center columns) or 48 h (right column) after plating in 0.3% FBS. Composite micrographs containing both vinculin (in black) and fibronectin (in white) patterns (*VN·FN* in plates *D–F*), or focal contacts (in black) and fibronectin fibers (in white) (*IR·FN* in plates *J–L*) show that *VN* striae, *FN* fibers, and very long focal contacts are all precisely coincident (see corresponding arrowheads in left and middle columns). Arrows in left column show a fiber continuously positive for vinculin (*A*) coincident with a long stria of fibronectin (*G*) and a long linear focal contact (*M*). Shorter vinculin-positive focal contacts near the edge of the cell were not labeled with fibronectin although their proximal ends were aligned with the distal termini of *FN* fibers (corresponding arrowheads, right column). Micrographs at right also depict interference-reflection bright fibers (*O*, short arrow) that are doubly labeled for fibronectin and vinculin (corresponding short arrows at right); these fibers were sometimes interference reflection-dark at one end and bright at the other (*O*, long arrow, and corresponding long arrows at right). Crossed arrows in *A*, *M*, *C*, and *O* indicate focal contacts which are only partially *VN*-labeled. White arrowheads in *D* and *J* show a close lateral apposition of *FN* fibers and *VN*+ focal contacts. × 1,350.

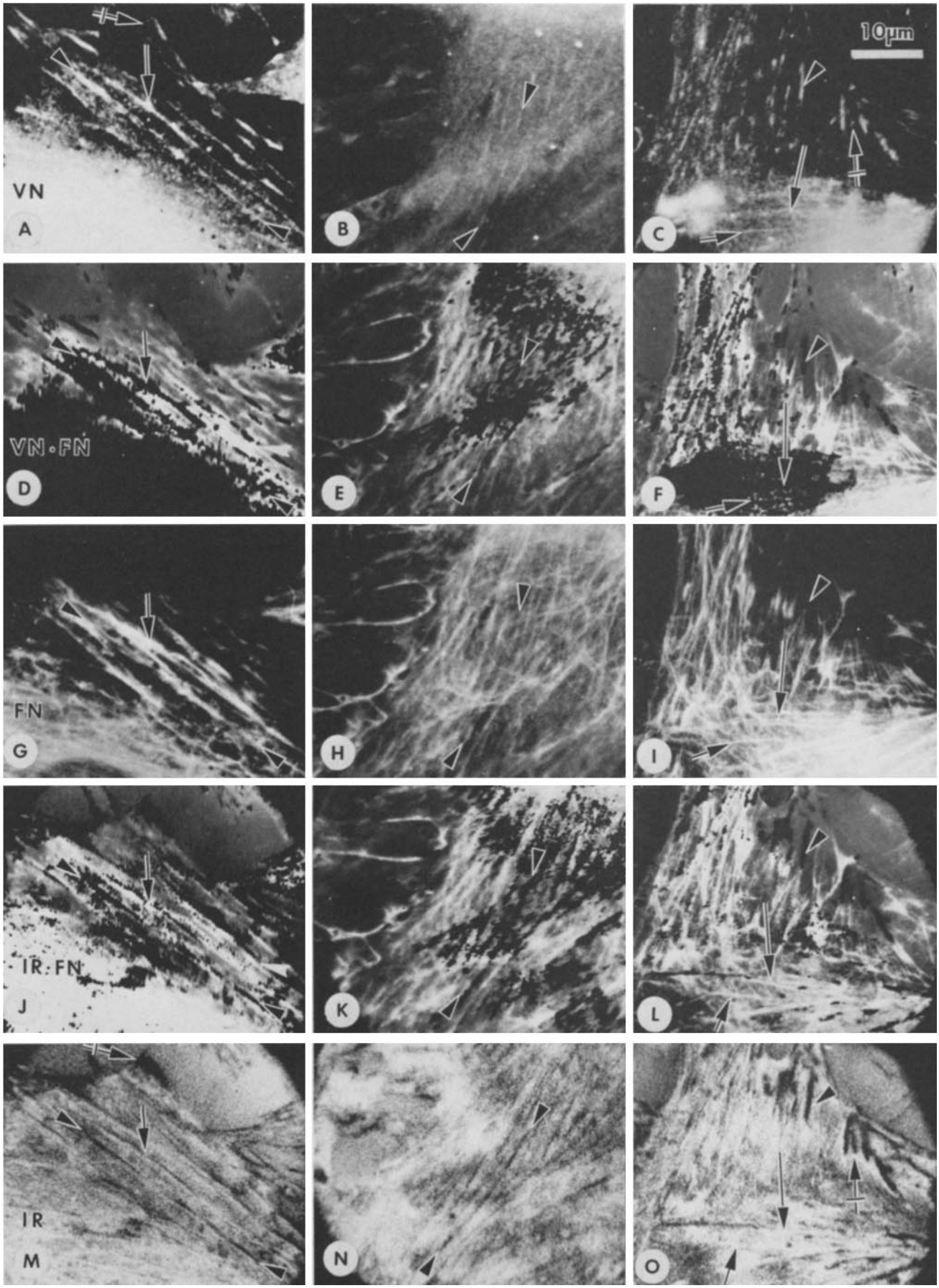
VN
A
B
10μm
C
VN·FN
D
E
F
FN
G
H
I
IR·FN
J
K
L
IR
M
N
O

Correspondence of Striae Containing Both Fibronectin and Vinculin with the Major Phase-Dense Stress Fibers at the Ventral Surface of Stationary Nil 8 Cells

Possible relationships between the ventral stress fibers and the very long focal contacts coincident with fibronectin and vinculin staining (Figs. 3 and 4) were assessed using the composite photomicrographic technique outlined in the previous section. Striae exhibiting fibronectin (indicated in white) and vinculin (shown reversed in black) coincidence were identified (Fig. 5 *D–F*) and their relationship to the phase morphology was then studied directly by placing a high contrast phase photomicrotransparency over the micrograph of FN immunofluorescence (Fig. 5 *J–L*). Phase-dense stress fibers (in black) were precisely coincident with striae that were doubly stained for both fibronectin (FN in white) and vinculin in 46 G_1-arrested Nil 8 fibroblasts studied from 24 to 72 h after seeding. The stress fibers usually were continuously stained with fibronectin antibodies (Fig. 5 *G–L*), but their vinculin labeling was either discontinuous (Fig. 5, left and center columns), resembling tandemly arranged focal contacts, or strikingly continuous (Fig. 5, right column).

DISCUSSION

In this study and our previous report (45), we found vinculin localized in oblong focal patches and in longitudinal fibers which ran along the ventral fibroblast surface from the nucleus toward the cellular margin. Most of the elongated fibers, and many of the focal patches, were precisely superimposed upon extracellular fibronectin fibers as shown in double-label composite micrographs of well-spread growth-arrested Nil 8 cells. The observation that these regions of vinculin and fibronectin coincidence are dark under interference reflection microscopy is very significant because it indicates that this FN-VN association is indeed localized at the points of very close substrate apposition (approx. 15 nm) (34) in these flattened cells. The double-label composite method used to demonstrate this triple association was shown to reproduce accurately the relative distributions of fibronectin and vinculin striae with respect to focal contacts and stress fibers. Following the application of this technique, the mean percentage increase in fiber width found in the overlays or underlays was very small (~ 5%) and both values were not significantly different. Therefore, one would not expect this procedure to produce an artificial coincidence between unrelated structures, and comparative measurements on the original micrographs support this expectation. To further test the reliability of the double-label composite method, I performed two independent superimposition combinations for each fibronectin underlay: one overlay derived from the corresponding vinculin pattern (*D–F* in Figs. 3–5), and the other from the matching IRM or phase pattern (*J–L* in Figs. 3–5). Because VN plaques are usually coincident with and thought to be a component of focal contacts (5, 21, 22), and because focal contacts are coincident with the termini of phase-dense stress fibers (28), both combinations should show the same close relationship between black overlay fibers (representing VN, focal contacts, or stress fibers) and the white fibronectin striae of the underlay. The series *D–F* and *J–L* in Figs. 3–5 do indeed demonstrate a consistent superimposition of VN fibers, focal contacts, and stress fibers upon fibronectin striae. The application of this method therefore enables one to accurately study the relationships of two immunolabels with IRM minima or phase-dense structures simultaneously over a large cellular area. I also believe that the longitudinal perinuclear interference reflection minima represent focal contacts for the following reasons: (*a*) changes in cell thickness from values >1 μm through values <1 μm measured by electron microscopy of transverse sections had no effect upon the IRM pattern produced with an I.N.A. of 1.25; (*b*) the minima contained many areas that were as dark as the more typical focal contacts and exhibited a rather straight elongated morphology oriented normal to the cell margin; (*c*) no fringelike minima similar in shape to the cell margin and oriented parallel to it were ever observed in the perinuclear region; (*d*) the elongate fibrous patterns of vinculin, which has been shown to be localized in focal contacts (5, 21), were precisely coincident with these perinuclear IR minima (Figs. 3 *A*, *B* and *M*, *N*; 4 *A*, *C* and *M*, *O*). The fibronectin- and vinculin-positive fibers and

FIGURE 4 Vinculin (*VN* in plates *A–C*) and fibronectin (*FN* in plates *G–I*) striae are located at focal contacts (interference-reflection micrographs *M–O*) of doubly stained Nil 8 cells arrested in 0.3% FBS for 48 h (left and center columns) or for 72 h (right column). Double composite micrographs of photographically reversed vinculin immunolabeling (indicated in black) and anti-fibronectin staining (in white) are shown in plates *D–F* (*VN·FN*). Similar photomicrographic combinations consisting of focal contacts (in black) derived from the corresponding interference reflection micrographs, and of fibronectin fibers (in white) are presented in plates *J–L* (*IR·FN*). Left Column (48 h): Pairs of arrowheads pinpoint the termini of two long fibronectin fibers extending from the perinuclear area to the cell margin (*G*). Vinculin striae (*A*, arrowheads), which superimpose elongated focal contacts (*M*, arrowheads), are coincident with the distal half of the upper *FN* fiber and all but the midpoint of the lower one (*D*, *J* matching arrowheads). The relationship between *FN*, *VN*, and focal contacts is sometimes a close lateral apposition (*D*, *J* white arrowheads). A shorter *FN* fiber (*G*) whose end is shown by the top of the lower case e is strikingly congruent with vinculin staining (*A*, *D*) and a focal contact (*J*, *M*). The bottom of the e is located above the ends of two similar FN fibers (in *G*) which are coincident with the proximal halves of two long vinculin-containing focal contacts (corresponding e's at left). A focal contact negative for both *FN* and *VN* is indicated by the matching arrows at the cell margin. Center Column (48 h): These micrographs show the edges of two cells (seen most clearly in *B* and *N*) which are overlapped by fibronectin fibers (*H*). Matching arrows indicate two triangular clusters of focal contacts at the cell margins which are doubly labeled for fibronectin and vinculin. Proximal termini of the longer focal contacts (*N*, corresponding pairs of arrowheads) contain both *FN* and *VN* staining, with the fibronectin fiber extending farther toward the upper cell center (*E*). Right Column (72 h): Upper arrowhead (*O*) shows a short perinuclear focal contact containing fibronectin (*F*, *I*, *L*) and vinculin (*C*, *F*). A similar *FN*-labeled focal contact is indicated by the corresponding lower arrowheads. Beneath the latter adhesion is a longer focal contact heavily labeled with fibronectin antibody for one-third of its proximal length (*P*) and at its distal tip, with less intense anti-*FN* staining along the rest of its expanse (*I*). Most of the *FN* labeling is coincident with vinculin staining in this focal contact (*C*, *F*). A vinculin-positive focal contact (*C*, large arrow) situated farther away from the nucleus is tandemly aligned with a fiber of fibronectin, but the main body of this adhesion lacks fibronectin (*I*). The matching short arrows depict three oblong focal contacts near the edge of the cell which do not contain *FN* or *VN*. × 1,200.

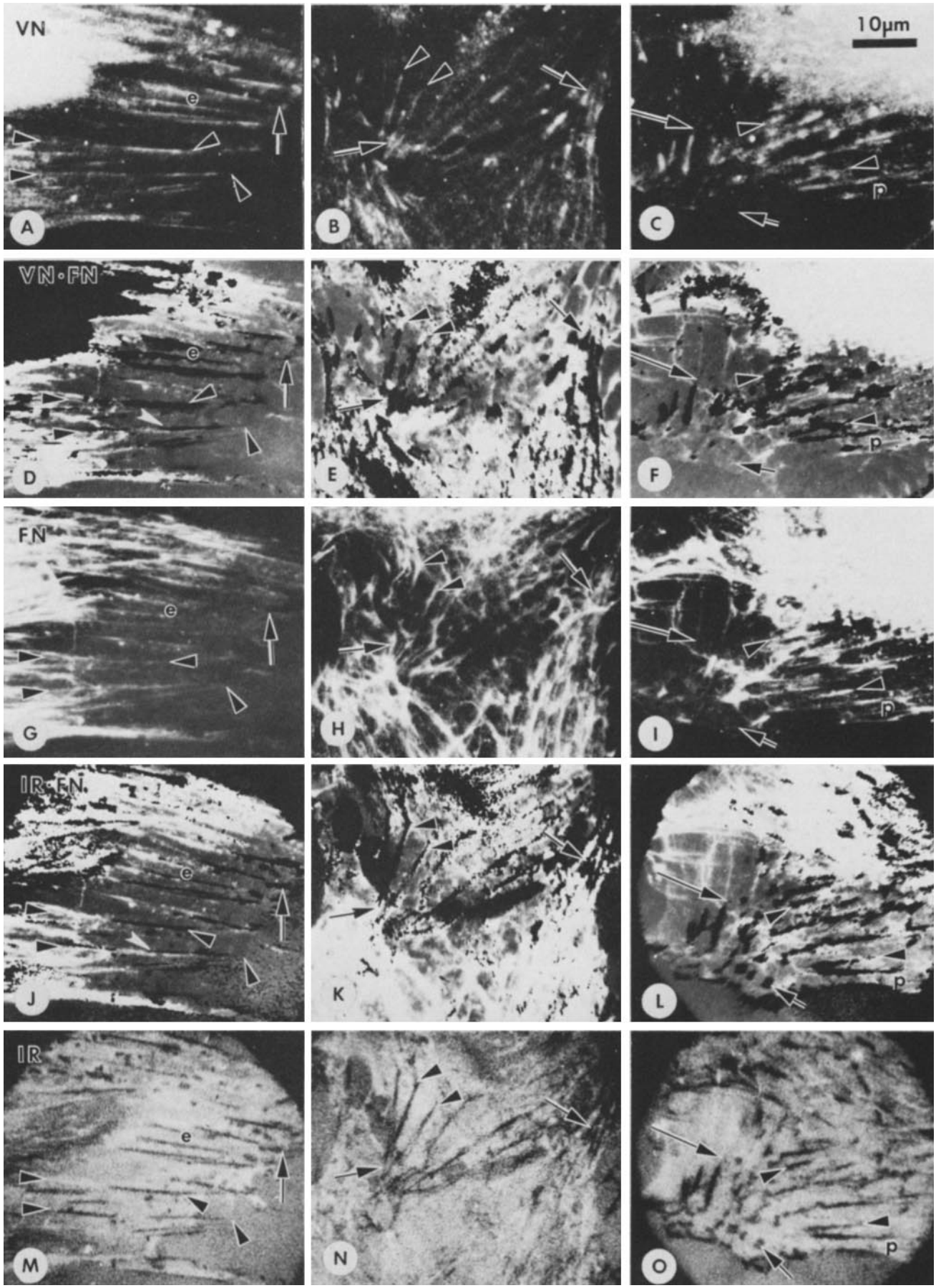
VN
e
A
B
10μm
P
C
VN•FN
e
D
E
P
F
FN
e
G
H
P
I
IR•FN
e
J
K
P
L
IR
e
M
N
P
O

focal patches that were coincident with dark IRM minima are thus focal contacts that contain fibronectin. Furthermore, this conclusion is supported by recent experiments in this laboratory that demonstrate that fibronectin fibers reconstituted on the ventral surfaces of HSV-transformed Nil fibroblasts maintained in 0.3% FBS are also coincident with focal contacts.[1]

Using phase-contrast microscopy, we have also established that longitudinal fibronectin- and vinculin-positive fibers are coincident with the major ventral phase-dense stress fibers. These FN- and VN-containing fibers are apparently different from the ones observed at the dorsal cell surface (11). Since vinculin has been precisely localized in the membrane insertion sites of actin microfilament bundles (termini of stress fibers) (11, 21, 22), our observation of antivinculin staining along nearly the entire length of the stress fibers (Figs. 1 *C*, 3 *A*, and 5 *C*) suggests that they are situated close to the inner surface of the plasmalemma along most of their longitudinal expanse in sessile fibroblasts. Composite micrographs depicting the interference reflection patterns of these VN- and FN-positive fibers reveal that they are also reflection negative (dark) for most of their length, indicating that they are closely apposed to the substrate (≃15 nm) (Figs. 1 *B* and 3 *M*). Our results thus intimate that, besides their reputed role of drawing the cell body forward during cellular locomotion (2, 35), the stress fibers probably function predominantly as very long substrate adhesion complexes in well-spread stationary fibroblasts. Also, Hynes has recently observed that many actin bundles that overlap FN fibers are coincident with focal contacts (32). These data collectively suggest that the ventral fibronexus, defined as the transmembrane association of actin, vinculin, and fibronectin (44, 45), is localized at the sites of closest substrate approach (≃15 nm) during stationary culture conditions.

It should be noted that not all of the focal contacts detected by IRM were positive for fibronectin and/or vinculin. Oblong VN-negative focal contacts were found at the edges of cells cultured in either high or low concentrations of serum. Although vinculin was localized in the more centripetal focal contacts of these cells, fibronectin fibers were unrelated to them until 24 h after seeding in media with low serum concentrations. By this time, the pattern of fibronectin fibers became much more linear, and these FN fibers were then coincident with VN-positive focal contacts and VN-positive stress fibers that were interference-reflection negative. The presence of FN-positive, VN-positive, and interference reflection-negative fibers was most striking in the perinuclear area; they were seen less frequently toward the cellular periphery. We hypothesize that these several kinds of focal contacts represent different stages in the development of a mature substrate adhesion complex. Because new focal contacts are always generated at the distal margin of the cell (35), the sequence of events which we report suggests that the development of the perinuclear adhesion complexes follows this temporal and spatial course: (*a*) the youngest focal contacts which form at the very edge of the cell are VN-negative, FN-negative; (*b*) intermediate focal contacts located more centrally are VN-positive, FN-negative; (*c*) perinuclear focal contacts and stress fibers which are VN-positive, FN-positive, and interference-reflection negative represent the full-blown substrate adhesion complex. The association of fibronectin with focal contacts might stabilize them in stationary flattened fibroblasts.

Cells cultured in high concentrations of serum (5% FBS) showed good correspondence between VN and focal contacts, but most of the contacts were plaquelike rather than long and fibrous as observed in the G_1-arrested fibroblasts, suggesting that the adhesive properties of these two systems differ. Another important difference is that few fibronectin fibers were coincident with the focal contacts of the high-serum cultures during the entire 72-h observation period. These results are in agreement with a number of recent studies reporting that FN is absent from many focal contacts, because all of these experiments were performed in serum concentrations of 5% or greater (5, 6, 8, 13, 20). We attribute the lack of fibronectin-focal contact coincidence to the heightened surface activity and the rapid flux of focal contacts observed in cultures supplemented with high serum levels or mitogens (5, 9, 18, 35, 45). The focal contact should therefore be considered as a dynamic structure whose chemical composition is very sensitive to the particular state of cellular motility. Fibronectin-negative focal contacts may be the least stable type of adhesion site characteristic of motile cells, whereas G_1-arrested stationary cells probably possess fibronectin beneath their focal contacts and stress fibers to augment their substrate attachment. It is important to mention that many cell types that are not usually exposed to high serum levels are attached to fibronectin-containing basement membranes in vivo (15, 47); they might use fibronectin- and vinculin-containing adhesion complexes similar to those described in our stationary cultures to maintain a stable tissue organization.

The localization of both vinculin and fibronectin in focal contacts of quiescent cells also has some bearing on the mechanism whereby the transformed phenotype is expressed. Many types of transformed cells exhibit reduced quantities of microfilament bundles (4, 24, 48) and are deficient in binding fibronectin fibers to their external surfaces (4, 12, 38, 46). Recently, p60src protein, the gene product responsible for maintaining the transformed phenotype in Rous sarcoma virus-transformed cells (27), also has been localized in the focal contacts (40). The p60src protein appears to exert its transforming action by increasing the intracellular levels of phosphorylated proteins (43), and vinculin is apparently one of the substrates for this action in the RSV system (42). Increased phosphorylation of vinculin might disrupt the association of

[1] Singer, I. I. Fibronexus formation is an early event during fibronectin induced restoration of a more normal morphology and substrate adhesion pattern in transformed hamster fibroblasts. Manuscript in preparation.

FIGURE 5 Major ventral stress fibers (arrowheads in phase micrographs *M–O*) of sessile Nil 8 fibroblasts arrested in 0.3% FBS are coincident with striae exhibiting both vinculin (*VN*; corresponding arrowheads in *A–C*) and fibronectin (*FN*; matching arrowheads in *G–I*) immunolabeling. Combination photomicrographs depicting the superimposition of vinculin (in black) and fibronectin (in white) at these striae (arrowheads) are shown in *D–F* (*VN·FN*). Photographic composites of phase-dense structures (which display stress fibers and the cellular margins in black), plus the underlying fibronectin fibers (in white) (*PH·FN*), show that the fibronectin striae, which are overlapped by vinculin staining, are coincident with stress fibers (arrowheads in *J–L*). Left and Middle Columns (48 h): The vinculin patterns along fibronectin-coincident stress fibers (matching arrowheads) appear discontinuous, resembling linear arrangements of focal patches. Right Column (72 h): Phase-dense stress fibers appear continuously labeled with vinculin and fibronectin (matching arrowheads). × 1,100.

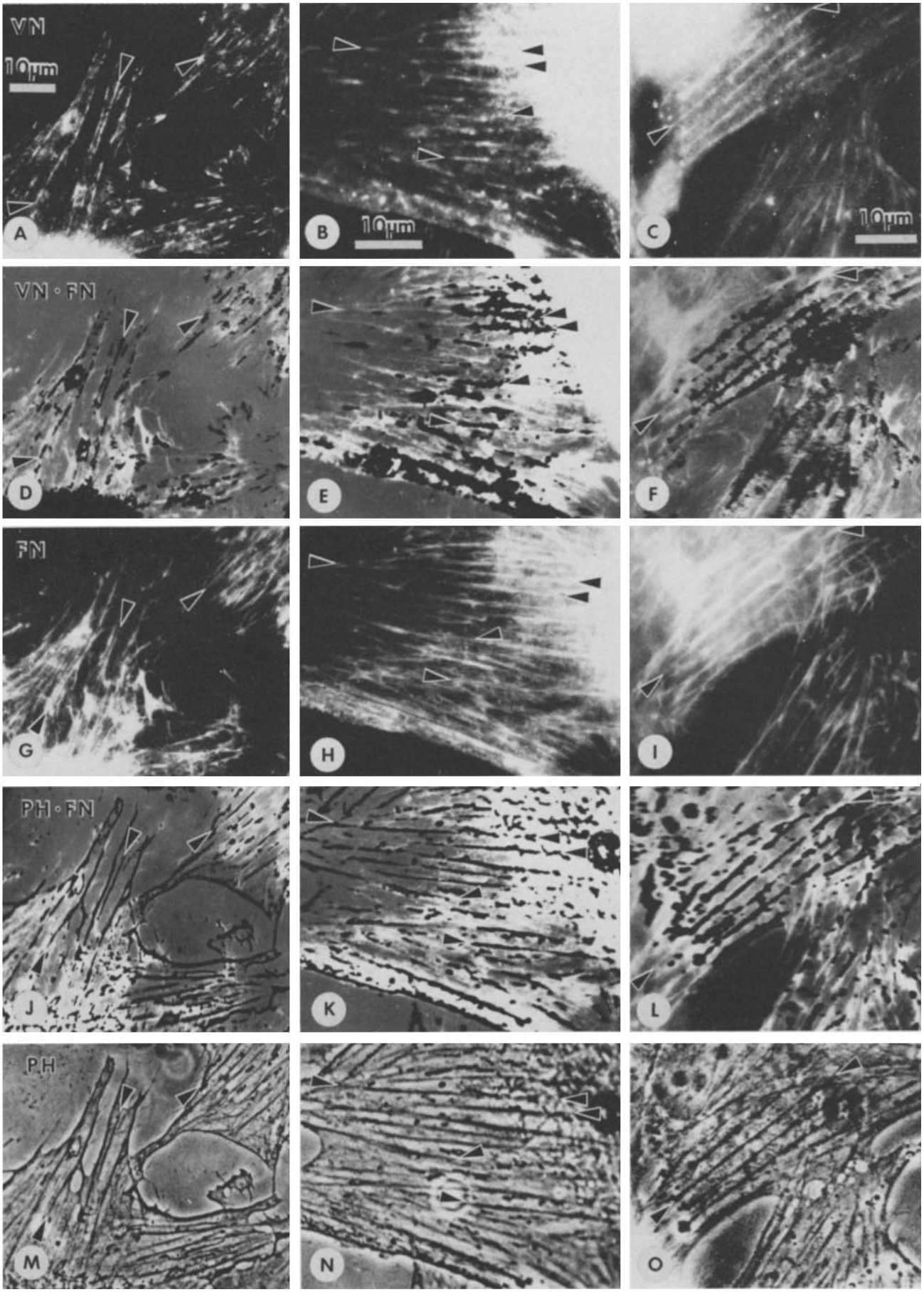
VN
10μm
A
B
10μm
C
10μm
VN • FN
D
E
F
FN
G
H
I
PH • FN
J
K
L
PH
M
N
O

microfilament bundles and fibronectin fibers within focal contacts, resulting in the decreased substrate adhesion and rounded morphology characteristic of oncorna virus-transformed cells (31). The same argument may be applied to fibronectin, which exhibits higher levels of phosphorylation in transformed cells as compared with normal ones (3).

I thank Robert L. Costantino and M. Suzanne Hopkins for expert technical assistance, and Dr. Richard O. Hynes for explaining how to perform interference reflection microscopy with the American Optical epifluorescence microscope. Useful discussions were also held with Drs. R. O. Hynes, C. S. Izzard, P. R. Paradiso, and S. L. Rhode III. The comments of the reviewers have helped to improve this manuscript. Mrs. V. Haas patiently typed this manuscript.

This work was supported by grant 1 RO1 CA27389-02 to Dr. I. I. Singer from the U. S. Public Health Service, National Cancer Institute, and by generous gifts from the Nichols Foundation and Mrs. Sarah Given Larson.

Received for publication 20 May 1981, and in revised form 25 August 1981.

REFERENCES

1. Abercrombie, M., and G. A. Dunn. 1975. Adhesions of fibroblasts to substratum during contact inhibition observed by interference reflection microscopy. *Exp. Cell Res.* 92:57–62.
2. Abercrombie, M., J. E. M. Heaysman, and S. M. Pegrum. 1971. The locomotion of fibroblasts in culture. IV. Electron microscopy of the leading lamella. *Exp. Cell Res.* 67: 359–367.
3. Ali, I. U., and T. Hunter. 1981. Structural comparison of fibronectins from normal and transformed cells. *J. Biol. Chem.* 256:7671–7677.
4. Ali, I. U., V. Mautner, R. Lanza, and R. O. Hynes. 1977. Restoration of normal morphology: adhesion and cytoskeleton in transformed cells by addition of a transformation-sensitive surface protein. *Cell.* 11:115–126.
5. Avnur, Z., and B. Geiger. 1981. The removal of extracellular fibronectin from areas of cell-substrate contact. *Cell.* 25:121–132.
6. Badley, R. A., A. Woods, C. G. Smith, and D. A. Rees. 1980. Actomyosin relationships with surface features in fibroblast adhesion. *Exp. Cell Res.* 126:263–272.
7. Bloch, R. J., and B. Geiger. 1980. The localization of acetylcholine receptor clusters in areas of cell-substrate contact in cultures of rat myotybes. *Cell.* 21:25–35.
8. Birchmeier, C., T. E. Kreis, H. M. Eppenberger, K. H. Winterhalter, and W. Birchmeier. 1980. Corrugated attachment membrane in WI-38 fibroblasts: alternating fibronectin fibers and actin-containing focal contacts. *Proc. Natl. Acad. Sci. U. S. A.* 77:4108–4112.
9. Brunk, U., J. Schellens, and B. Westermark. 1976. Influence of epidermal growth factor (EGF) on ruffling activity, pinocytosis, and proliferation of cultivated human glia cells. *Exp. Ceil Res.* 103:295–302.
10. Burridge, K. 1976. Changes in cellular glycoproteins after transformation: identification of specific glycoproteins and antigens in sodium dodecyl sulfate gels. *Proc. Natl. Acad. Sci. U. S. A.* 73:4457–4461.
11. Burridge, K., and J. R. Feramisco. 1980. Microinjection and localization of a 130K protein in living fibroblasts: a relationship to actin and fibronectin. *Cell.* 19:587–595.
12. Chen, L. B., P. H. Gallimore, and J. K. McDougall. 1976. Correlation between tumor induction and the large external transformation sensitive protein on the cell surface. *Proc. Natl. Acad. Sci. U. S. A.* 73:3570–3574.
13. Chen, W.-T., and S. J. Singer. 1980. Fibronectin is not present in the focal adhesions formed between normal cultured fibroblasts and their substrata. *Proc. Natl. Acad. Sci. U. S. A.* 77:7318–7322.
14. Couchman, J. R., and D. A. Rees. 1979. The behavior of fibroblasts migrating from chick heart explants: changes in adhesion, locomotion, and growth, and in the distribution of actomyosin and fibronectin. *J. Cell Sci.* 39:149–165.
15. Courtoy, P. J., Y. S. Kanwar, R. O. Hynes, and M. G. Farquhar. 1980. Fibronectin localization in the rat glomerulus. *J. Cell Biol.* 87:691–696.
16. Critchley, P. R., K. A. Chandrabose, J. M. Graham, and I. A. Macpherson. 1974. Glycolipids in Nil hamster cells as a function of cell density and cell cycle. *In:* Control of Cell Proliferation. B. Clarkson and R. Baserga, editors. Cold Spring Harbor Laboratory, Cold Spring Harbor, N. Y. 481–493.
17. Curtis, A. S. G. 1964. The mechanism of adhesion of cells to glass. *J. Cell Biol.* 20:199–215.
18. Evans, R. B., V. Morhenn, A. L. Jones, and G. M. Tomkins. 1974. Concomitant effects of insulin on surface membrane conformation and polysome profiles of serum starved Balb/C 3T3 fibroblasts. *J. Cell Biol.* 61:95–106.
19. Feramisco, J. R. and K. Burridge. 1981. A rapid purification of α-actinin, filamin, and a 130,000-dalton protein from smooth muscle. *J. Biol. Chem.* 255:1194–1199.
20. Fox, C. H., M. H. Cottler-Fox, and K. M. Yamada. 1980. The distribution of fibronectin in attachment sites of chick fibroblasts. *Exp. Cell Res.* 130:477–481.
21. Geiger, B. 1979. A 130K protein from chicken gizzard: its localization at the termini of microfilament bundles in cultured chicken cells. *Cell.* 18:193–205.
22. Geiger, B., K. T. Tokuyasu, A. H. Dutton, and S. J. Singer. 1980. Vinculin, an intracellular protein localized at specialized sites where microfilament bundles terminate at cell membranes. *Proc. Natl. Acad. Sci. U. S. A.* 77:4127–4131.
23. Gingell, D. 1981. The interpretation of interference-reflection images of spread cells: significant contributions from thin peripheral cytoplasm. *J. Cell Sci.* 49:237–247.
24. Goldman, R. D., M.-J. Yerna, and J. A. Schloss. 1976. Localization and organization of microfilaments and related proteins in normal and virus-transformed cells. *J. Supramol. Struct.* 5:155–183.
25. Grinnel, F., and M. K. Feld. 1979. Initial adhesion of human fibroblasts in serum-free medium: possible role of secreted fibronectin. *Cell.* 17:117–129.
26. Haemmerli, G., P. Sträüli, and J. S. Ploem. 1980. Cell-to-substrate adhesions during spreading and locomotion of carcinoma cells. *Exp. Cell Res.* 128:249–256.
27. Hanafusa, H. 1977. Cell transformation by RNA tumor viruses. *In:* Comprehensive Virology. H. Fraenkel-Conrat and R. R. Wagner, editors. Plenum Press, N. Y. Vol. 10. 401–483.
28. Heath, J. P., and G. A. Dunn. 1978. Cell-to-substratum contacts of chick fibroblasts and their relation to the microfilament system. A correlated interference-reflexion and high voltage electron-microscope study. *J. Cell Sci.* 29:197–212.
29. Heaysman, J. E. M., and S. M. Pegrum. 1973. Early contacts between fibroblasts, an ultrastructural study. *Exp. Cell Res.* 78:71–78.
30. Heggeness, M. H., J. F. Ash, and S. J. Singer. 1978. Transmembrane linkage of fibronectin to intracellular actin-containing filaments in cultured human fibroblasts. *Ann. N. Y. Acad. Sci.* 312:414–417.
31. Hynes, R. O. 1980. Cellular location of viral transforming proteins. *Cell.* 21:601–602.
32. Hynes, R. O. 1981. Relationships between fibronectin and the cytoskeleton. *In:* Cell Surface Reviews, Vol. 7 Cytoskeletal Elements and Plasma Membrane Organization. G. Poste and G. L. Nicolson, editors. In press.
33. Hynes, R. O., and A. T. Destree. 1978. Relationships between fibronectin (LETS protein) and actin. *Cell.* 15:875–886.
34. Izzard, C. S., and L. R. Lochner. 1976. Cell-to-substrate contacts in living fibroblasts: an interference reflexion study with an evaluation of the technique. *J. Cell Sci.* 21:129–159.
35. Izzard, C. S., and L. R. Lochner. 1980. Formation of cell-to-substrate contacts during fibroblast motility: an interference-reflexion study. *J. Cell Sci.* 42:81–116.
36. Kiebe, R. J. 1974. Isolation of a collagen dependent cell attachment factor. *Nature (Lond.).* 250:248–251.
37. Laemmli, U. K. 1970. Cleavage of structural proteins during the assembly of the head of bacteriophage T4. *Nature (Lond.).* 227:680–685.
38. Mautner, V., and R. O. Hynes. 1977. Surface distribution of LETS protein in relation to the cytoskeleton of normal and transformed cells. *J. Cell Biol.* 75:743–768.
39. Pearlstein, E. 1976. Plasma membrane glycoprotein which mediates adhesion of fibroblasts to collagen. *Nature (Lond.).* 262:497–500.
40. Rohrschneider, L. R. 1980. Adhesion plaques of Rous sarcoma virus-transformed cells contain the src gene product. *Proc. Natl. Acad. Sci. U. S. A.* 77:3514–3518.
41. Ruoslahti, E., M. Vuento, and E. Engvall. 1978. Interaction of fibronectin with antibodies and collagen in radioimmunoassay. *Biochim. Biophys. Acta.* 534:210–218.
42. Sefton, B. M., T. Hunter, E. H. Ball, and S. J. Singer. 1981. Vinculin a cytoskeletal target of the transforming protein of Rous sarcoma virus. *Cell.* 24:165–174.
43. Sefton, B. M., T. Hunter, K. Beemon, and W. Eckard. 1980. Evidence that the phosphorylation of tyrosine is essential for cellular transformation by Rous sarcoma virus. *Cell.* 20: 807–816.
44. Singer, I. I. 1979. The fibronexus: a transmembrane association of fibronectin-containing fibers and bundles of 5 nm microfilaments in hamster and human fibroblasts. *Cell.* 16: 675–685.
45. Singer, I. I., and P. R. Paradiso. 1981. A transmembrane relationship between fibronectin and vinculin (130Kd protein): serum modulation in normal and transformed hamster fibroblasts. *Cell.* 24:481–492.
46. Smith, H. S., J. L. Riggs, and M. W. Mosesson. 1979. Production of fibronectin by human epithelial cells in culture. *Cancer Res.* 39:4138–4144.
47. Stenman, S., and A. Vaheri. 1978. Distribution of a major connective tissue protein, fibronectin, in normal human tissues. *J. Exp. Med.* 147:1054–1064.
48. Tucker, R. W., K. K. Sanford, and F. R. Frankel. 1978. Tubulin and actin in paired non-neoplastic and spontaneously transformed neoplastic cell lines in vitro: fluorescent antibody studies. *Cell.* 13:629–642.
49. Wehland, J., M. Osborn, and K. Weber. 1979. Cell-to-substratum contacts in living cells: a direct correlation between interference-reflexion and indirect immunofluorescence microscopy using antibodies against actin and α-actinin. *J. Cell. Sci.* 37:257–273.
50. Yamada, K. M., S. Yamada, and I. Pastan. 1976. Cell surface protein partially restores morphology, adhesiveness, and contact inhibition of movement to transformed fibroblasts. *Proc. Natl. Acad. Sci. U. S. A.* 73:1217–1221.